Molecular Crystals and Liquid Crystals Science and Technology. Section A. Molecular Crystals and Liquid Crystals
Publication details, including instructions for authors and subscription information:
http://www.tandfonline.com/loi/gmcl19

Tilt Angle Variation as a Function of Chain Length and Temperature in the Smectic C Phases of p, Alkoxyphenyl-p, Alkoxybenzoates

B. Heinrich [a] & D. Guillon [a]
[a] Institut de Physique et Chimie des Matériaux de Strasbourg, Groupe des Matériaux Organiques, 23, rue due Loess, B.P. 20CR, 67037, STRASBOURG Cedex, France
Version of record first published: 24 Sep 2006.

To cite this article: B. Heinrich & D. Guillon (1995): Tilt Angle Variation as a Function of Chain Length and Temperature in the Smectic C Phases of p, Alkoxyphenyl-p, Alkoxybenzoates, Molecular Crystals and Liquid Crystals Science and Technology. Section A. Molecular Crystals and Liquid Crystals, 268:1, 21-43

To link to this article: http://dx.doi.org/10.1080/10587259508030990

Mol. Cryst. Liq. Cryst., 1995, Vol. 268, pp. 21–43
Reprints available directly from the publisher
Photocopying permitted by license only

Tilt Angle Variation as a Function of Chain Length and Temperature in the Smectic C Phases of *p*, Alkoxyphenyl-*p*, Alkoxybenzoates

B. HEINRICH and D. GUILLON

Institut de Physique et Chimie des Matériaux de Strasbourg,
Groupe des Matériaux Organiques 23, rue due Loess, B. P. 20CR
67037 STRASBOURG Cedex- France

(Received October 18, 1994)

The variation of the tilt angle with temperature in the smectic C phase has generally been shown to be non-existent or very slow for compounds or mixtures with the nematic-smectic C transition, while in the case of systems with the smectic A- smectic C transition, a relation between the steepness of this variation, near the transition, and the width of the smectic A domain has been observed. In this work, the variation of tilt angle in the smectic C phase is described for *p*-alkoxyphenyl-*p*-alkoxybenzoate homologous series, for which the evolution of polymorphism can be controlled systematically, by varying stepwise the length of the aliphatic chains, and for which large domains can be obtained for each type of phase sequence, nematic-, smectic A- and isotropic- smectic C. After completing the discussion made previously on the incidence of chain length on polymorphism, we confirm that the variation of tilt angle with temperature is slowest for compounds with intermediate chain lengths corresponding to the largest smectic A temperature range; this variation becomes continuously steeper when the smectic A domain becomes narrow. In addition, we show that the same description can be extended to the other types of phase sequences, by using the hypothesis of a virtual smectic A-smectic C transition above the observed nematic- or isotropic-smectic C transition. In fact, short chain lengths for homologues with a nematic/smectic C transition, or long chain lengths for homologues with an isotropic/smectic C transition, lead to an increase of the tilt angle at the phase transition and to a decrease of the amplitude of its variation with temperature; in our description, this behaviour corresponds to an increase of the temperature range between the real and virtual transitions. As a consequence, the homologues with very short and very long chain lengths show a quasi temperature-independent tilt angle, while the other homologues present a tilt angle variation similar to that observed for compounds exhibiting a smectic C/smectic A transition. This feature indicates that there is no need to distinguish between different types of smectic C phase.

INTRODUCTION

Since the discovery of the smectic C phase in the late 60s, a lot of work has been done, using various techniques and compounds, in order to describe the dependence of tilt angle (ψ) as a function of temperature (T). Early studies indicated a strong correlation between the variation of ψ and the polymorphism, leading to the definition of two types of smectic C (S_C) phases[1] : the S_C phase, following a smectic A (S_A) phase, that would exhibit a tilt angle equal to zero at the transition, the tilt angle ψ then increasing continuously with decreasing T; and the S_C phase following a nematic (N) phase, that would exhibit higher values of ψ with no temperature dependence. Although the description of binary systems showing a complete miscibility of these "two types of

phases" made this distinction senseless [2], further studies have generally confirmed the correlation between the temperature dependence of ψ and the polymorphism.[3] However, for some compounds with the N-S_C phase sequences, a small variation of the high non-zero value of ψ with T has been clearly observed.[4] In order to follow the changeover between these two types of ψ variation with T, tilt angle variation studies close to the phase boundary in systems with a N-S_A-S_C triple point have been performed; they showed in particular an increase of the rate of variation of ψ with T near the transition when the S_A domain becomes smaller.[5] Moreover, calculations on calorimetric data suggest the same behaviour for compounds with the I-S_A-S_C phase sequence.[6] Besides the fact that the temperature range exhibiting the S_C phase was in general only explored partially, the few compounds used were not chosen according to a systematic variation of the molecular structure, and the incidence of mixing effects was neglected; therefore it cannot be excluded that the observed/calculated correlation with the width of the S_A domain would hide a more relevant relationship. In addition, tilt angle measurements on isolated compounds with the N-S_C phase sequence are of poor significance, as there is no easy parameter (like the width of the S_A domain), which could distinguish them, and there is a lack of studies on compounds with the I-S_C phase sequence. So, we think there was a real need for tilt angle measurements made on series of compounds, by varying systematically both the temperature and the molecular structure, in order to establish new relations, like that suggested with polymorphism, and to induce some evolution of the models describing the tilting in the S_C phase.

The most relevant molecular feature to vary is certainly the length of the aliphatic chains linked to the calamitic rigid core, since this parameter has a great (and roughly known) effect on the polymorphism, and since models usually describe tilting as the result of the packing of the rigid cores in the smectic layers. Furthermore, the chain length can be varied stepwise with a modest investment of chemistry, in contrast to other molecular features. In order to be as general as possible, we have chosen a very classical calamitic rigid core to perform this study, e.g. the 4-oxyphenyl-4′-oxybenzoate; the different homologues prepared are designated in the following by "*n*OPEPO*m*", where *n* and *m* are the number of carbon atoms of the linear aliphatic chains attached to the acid and to the phenol moiety, respectively:
This smectogenic C rigid core containing an ester function was preferred to similar ones

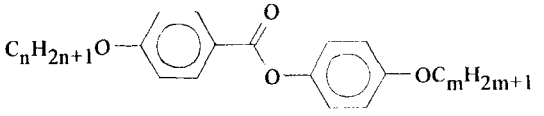

(with an imine or an azoxy function), because the final compounds have a high thermal stability and can be purified quite efficiently. In addition, results already published on some homologues, as well as empirical calculations[7], indicated that the systematic variation of *n* and *m* between 2 and 18 carbon atoms would lead to large areas of the *n*, *m*-plane corresponding to each type of phase sequence (I-N-S_C, I-N-S_A-S_C, I-S_A-S_C and I-S_C, "I" designating the isotropic phase). In this work, the *n* and *m* parameters were varied with an increment of 2, and only homologues with even values were investigated, in order to avoid any interaction with the odd-even effect. It has been observed that

quantities, like transition temperatures or smectic A layer spacings, show a smooth variation when the chain length is varied stepwise by two methylene groups, with a slight difference between the variations found for a total odd and even number of carbon atoms in the chain.[8] This small effect certainly deserves more detailed studies, which should enhance our understanding of molecular conformation and molecular packing in mesomorphic phases. These studies have to be performed with a systematic variation of chain length, the influence of total chain length and of chain asymmetry being compensated; furthermore, the non-equivalence of both ends of the rigid core should also be considered. Despite the fact that this extensive work should be clearly connected to the present work, we think it could be done independently and later on, so that, in this work, no influence of the odd-even effect could be detected since we have only considered the terms with the same parity of the carbon atom number in the aliphatic chains.

The results will be presented and discussed in two parts. In the first one, we will complete the description of the variation of the polymorphism in the (n, m) plane made earlier on the basis of empirical calculations. In the second one, we will discuss the variation of ψ as a function of n, m and of T, in relation with the variation of the polymorphism.

EXPERIMENTAL

The preparation and the characterisation of the materials are described in detail in appendix I. Some of the methods used in the present work were adapted from reference 14.

4-alkoxyphenols (2) (scheme 1) were prepared by O-alkylation from hydroquinone (**1**) with bromoalkanes and K_2CO_3 in cyclohexanone.

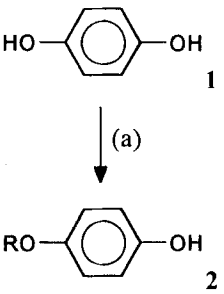

SCHEME 1 Reagents (a) RBr, K_2CO_3, CH_3COCH_3.

The 4-alkylphenols (**5**) (scheme 2) were prepared by a 2 step reaction: Friedel-Crafts acylation of phenol (**3**) followed by Clemmensen-reduction.

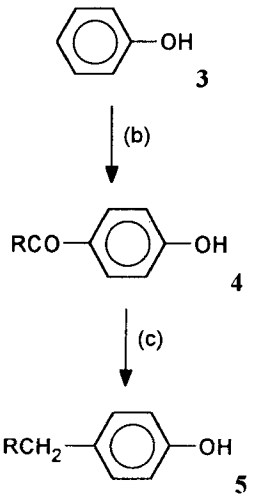

SCHEME 2 Reagents (b) RCOCl, $AlCl_3$, $C_6H_5NO_2$. (c) Zn-Hg, HCl, C_2H_5OH.

4-Alkoxybenzoic acids (**8**) (Scheme 3) were prepared from methyl *p*-hydroxybenzoate by a 2 step-reaction, composed of O-alkylation with bromoalkanes and K_2CO_3 in acetone and saponification with KOH in methanol-water.

Esters 9 were obtained (Scheme 3) by direct esterification using DCC (dicyclohexylcarbodiimide) and catalytic amounts of DMAP (4-dimethylaminopyridine). 4,4′-octyloxybiphenylcarboxylic acid (**14**) was prepared by a 4 step-reaction (scheme 4).

At first, 4, 4′-methoxycyanobiphenyl (**11**) was prepared from 4-methoxyphenyl zinc chloride (obtained from 4-bromoanisole (**10**)) and 4-bromocyanobenzene by Pd-coupling with $Pd[PPh_3]_4$ in THF. The ether group of **11** was cleaved with AlI_3 in acetonitrile.

Phenol 12 was O-alkylated with bromooctane, the conditions being the same as for step (d) in Scheme 3. Acid 14 was obtained by saponification with KOH in i-C_3H_7OH-water; the conversion to the amide was fast, but further conversion to the acid occured slowly. After chlorination of 14 with $SOCl_2$, the acid chloride and the phenols **5** were condensed, in the presence of pyridine to give the esters **15**.

^{1}H-NMR spectra were recorded using a Bruker 200 MHz FT NMR, and transition temperatures were measured using an Ortoplan Leitz-Wetzlar polarizing microscope with a Mettler FP80 hot stage. The tilt angle in the smectic C phase was calculated from the ratio of the smectic C layer spacing and of the layer spacing value extrapolated from the smectic A domain (see following section). The X-ray diffraction patterns have been obtained with a monochromatic and focused $CuK\alpha_1$ X-ray beam produced by a Philips generator, using the Guinier geometry, with samples filled into Lindemann capillaries.

To study the variations of the different properties investigated in this work (phase sequence width, tilt angle), we have used the (n, m) plane representation, where "iso" lines join virtual (n, m) pairs for which the property considered does not vary. These virtual (n, m) pairs have been obtained, after smoothing, from the different representations of the properties as a function of n or m. The relevance of the method has been demonstrated earlier, since fitting and extrapolation of the variations of transition temperatures, for homologues already prepared, permitted to predict polymorphism

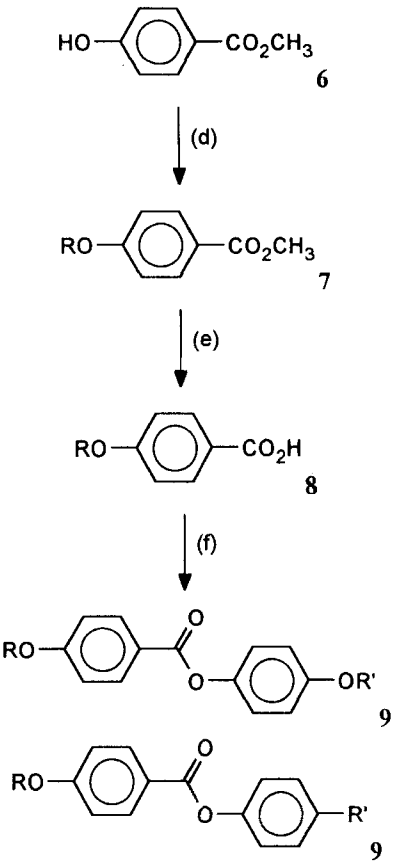

SCHEME 3 Reagents (d) RBr, K_2CO_3, CH_3COCH_3. (e) KOH, CH_3OH-H_2O (f) ROPhOH or RPhOH, DCC, DMAP, CH_2Cl_2.

and transition temperatures for some other terms[7]. Further confirmation of the relevance of the method lies in the fact that the predictions made for the whole liquid-crystalline (n, m) domain are in good agreement with our results. In addition, mixtures of neighbouring homologues, with $(n + m)$ values not differing by more than two units[9], have been used to check the position of the phase boundaries and of the "iso" lines for tilt angle (in the following called "equitilting" lines), in the portions of the (n, m) plane where the density of these lines was high*.

* The basic experimental results consist in 18 graphs representing the variation of transition temperatures as a function of n and m, and in 81 graphs representing the tilt angle variation as a function of T; in that way, it is not easy to present all the informations they contain. As a consequence, the (n, m) values corresponding to a given value of transition temperature, or to a given value of tilt angle, were reported in the (n, m) diagrams for some constant ΔT values and joined by a line before incrementing the given values. The location of the phase boundaries in the (n, m) plane was evaluated by extrapolating the transition temperatures and was corrected with mixtures of neighbouring molecules with $(n + m)$ not differing from more than two units (the mixing effects can then be neglected, as it will be shown in a forthcoming paper). A few mixtures were also studied by X-ray diffraction, in order to check the location of the « isotilting » lines when their density was high. Finally, the experimental points were removed for the sake of clarity, and the diagram was rotated by 45° to get the (n, m) representation.

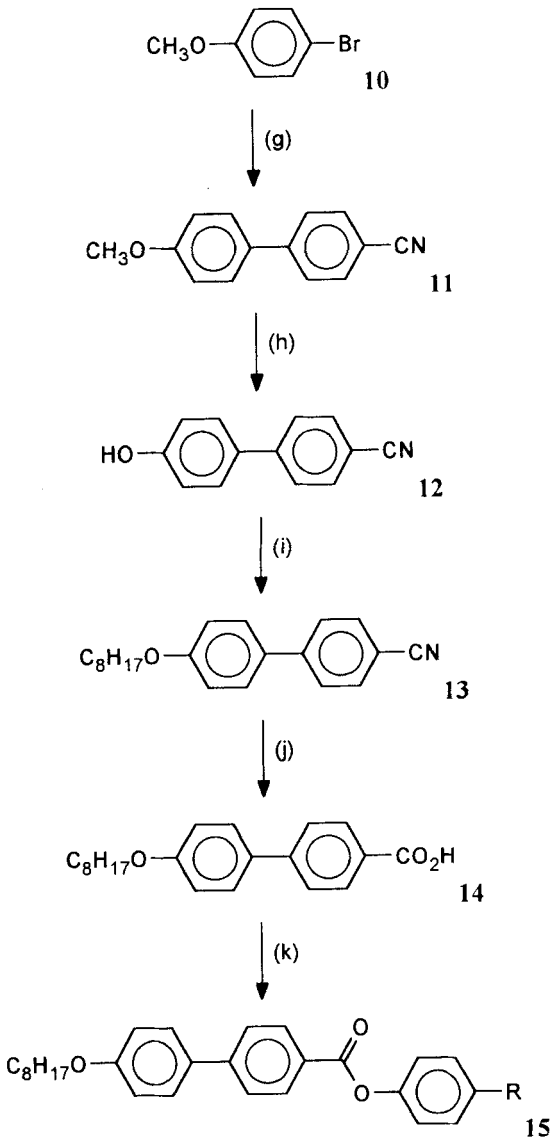

SCHEME 4 Reagents (g) Mg, THF–$ZnCl_2$, THF–BrPhCN, $Pd^{(0)}$ $[PPh_3]_4$, THF. (h) AlI_3, CH_3CN. (i) RBr, K_2CO_3, CH_3COCH_3. (j) KOH, $CH_3CHOHCH_3$–H_2O. (*k*) $SOCl_2$–RPhOH, Pyr–$PhCH_3$.

Of course, the tilt angle does not depend only upon n and m, but also upon temperature. As a consequence, we have drawn several figures representing the position of the equitilting lines, each of them for a different value of $\Delta T = T_{XC} - T$, T_{XC} being the transition temperature between the S_C phase and the high temperature phase ($X = A$ for smectic A, N for nematic and I for isotropic).

Finally, a diamond-shaped orientation of the (n,m) plane was chosen, in order to represent directly the results as a function of the total chain length $(n+m)$ and of the chain length asymmetry $|n-m|$, the $(n+m)$ and $|n-m|$ parameters being less interdependent than n and m alone, and more relevant for the discussion of the polymorphism and tilt angle variations.

RESULTS AND DISCUSSION

1. Polymorphism

The transition temperatures of all the compounds are reported in Table 1; polymorphism and transition temperatures are in good agreement with previous results[7]. A noteworthy feature lies in the fact that all the homologues exhibit at least one

TABLE I

Transition Temperatures (New Compounds are listed with bold characters; compounds reported in the literature are listed with italic characters)

Compound	K		S_B	S_C		S_A		N		I
2OPEPO2	●	115.3	–	–		–		●	116.0	●
2OPEPO4	●	102.8	–	–		–		●	107.4	●
2OPEPO6	●	80.1	–	–		–		●	94.5	●
2OPEPO8	●	83.6	–	–		–		●	92.1	●
2OPEPO10	●	88.9	–	–		–		(●)	88.8	●
2OPEPO12	●	92.2	–	–		–		(●)	85.7	●
2OPEPO14	●	95.7	–	–		–		(●)	83.7	●
2OPEPO16	●	98.9	–	(●)	76.8	–		(●)	82.6	●
2OPEPO18	●	104.4	–	(●)	78.2	–		(●)	79.9	●
4OPEPO2	●	96.8	–	–		–		●	97.5	●
4OPEPO4	●	86.4	–	–		–		●	91.4	●
4OPEPO6	●	64.8	–	–		–		●	88.7	●
4OPEPO8	●	65.7	–	–		–		●	88.2	●
4OPEPO10	●	75.2	–	–		–		●	85.0	●
4OPEPO12	●	78.1	–	–		–		●	81.7	●
4OPEPO14	●	80.8	–	–		–		(●)	80.2	●
4OPEPO16	●	83.6	–	–		–		(●)	78.9	●
4OPEPO18	●	86.7	–	–		–		(●)	70	●
6OPEPO2	●	77.7	–	–		–		●	93.9	●
6OPEPO4	●	69.2	–	–		–		●	88.2	●
6OPEPO6	●	62.4	–	–		–		●	87.9	●
6OPEPO8	●	52.8	–	(●)	47.6	–		●	88.9	●
6OPEPO10	●	61.0	–	(●)	54.5	–		●	86.9	●
6OPEPO12	●	66.8	–	(●)	59.7	–		●	84.7	●
6OPEPO14	●	72.4	–	(●)	62.2	–		●	82.5	●
6OPEPO16	●	80.3	–	(●)	63.8	–		●	80.8	●
6OPEPO18	●	83.4	–	(●)	65.2	–		(●)	79.2	●
8OPEPO2	●	79.2	–	–		–		●	93.8	●
8OPEPO4	●	62.8	–	(●)	58.5	–		●	89.8	●
8OPEPO6	●	51.8	–	●	65.9	–		●	89.7	●
8OPEPO8	●	55.7	–	(●)	73.4	–		●	90.5	●
8OPEPO10	●	65.0	–	●	78.7	–		●	90.1	●
8OPEPO12	●	68.9	–	●	80.1	●	81.6	●	88.5	●
8OPEPO14	●	71.4	–	●	79.6	●	83.2	●	86.2	●
8OPEPO16	●	76.0	–	●	78.5	●	83.6	●	84.9	●
8OPEPO18	●	81.1	–	(●)	77.4	●	83.4	●	83.7	●

TABLE I (*Continued.*)

Compound	*K*		S_B		S_C		S_A		*N*		*I*
10OPEPO2	●	79.4	–		–		(●)	65.4	●	90.9	●
10OPEPO4	●	56.4	–		●	57.8	●	79.1	●	87.9	●
10OPEPO6	●	60.1	–		●	77.0	●	82.2	●	88.0	●
10OPEPO8	●	63.2	–		●	84.8	●	87.0	●	90.6	●
10OPEPO10	●	72.9	–		●	87.7	●	88.5	●	89.8	●
10OPEPO12	●	75.2	–		●	87.5	●	88.3	–		●
10OPEPO14	●	78.5	–		●	86.8	●	88.1	–		●
10OPEPO16	●	78.2	–		●	84.8	●	87.1	–		●
10OPEPO18	●	85.4	–		(●)	83.7	●	85.4	–		●
12OPEPO2	●	76.1	–		–		(●)	74.9	●	88.8	●
12OPEPO4	●	67.3	(●)	51.2	–		●	81.6	–		●
12OPEPO6	●	68.4	(●)	56.3	●	78.2	●	87.8	–		●
12OPEPO8	●	69.5	(●)	60.2	●	89.1	●	91.2	–		●
12OPEPO10	●	79.9	(●)	60.9	●	91.4	–		–		●
12OPEPO12	●	82.0	(●)	61.5	●	90.4	–		–		●
12OPEPO14	●	84.1	(●)	62.9	●	90.0	–		–		●
12OPEPO16	●	87.3	(●)	67.3	●	88.2	–		–		●
12OPEPO18	●	88.4	(●)	70.2	(●)	87.4	–		–		●
14OPEPO2	●	78.4	–		–		●	78.8	(●)	87.5	●
14OPEPO4	●	77.4	(●)	61.4	–		●	86.5	–		●
14OPEPO6	●	76.6	(●)	65.6	●	74.8	●	88.1	–		●
14OPEPO8	●	73.8	(●)	70.0	●	90.3	●	91.5	–		●
14OPEPO10	●	83.8	(●)	71.0	●	91.9	–		–		●
14OPEPO12	●	85.7	(●)	71.5	●	91.2	–		–		●
14OPEPO14	●	89.9	(●)	72.2	●	90.9	–		–		●
14OPEPO16	●	92.7	(●)	75.1	(●)	90.1	–		–		●
14OPEPO18	●	93.2	(●)	78.7	●	89.6	–		–		●
16OPEPO2	●	80.6	–		–		●	81.1	●	85.6	●
16OPEPO4	●	82.6	(●)	66.4	–		●	86.1	–		●
16OPEPO6	●	81.3	(●)	71.4	–		●	88.3	–		●
16OPEPO8	●	77.4	(●)	76.9	●	90.5	●	91.3	–		●
16OPEPO10	●	84.2	(●)	78.2	●	91.2	–		–		●
16OPEPO12	●	86.6	(●)	79.3	●	91.1	–		–		●
16OPEPO14	●	90.4	(●)	80.3	●	90.6	–		–		●
16OPEPO16	●	92.9	(●)	82.2	(●)	89.7	–		–		●
16OPEPO18	●		(●)	84.8	(●)	89.4	–		–		●
18OPEPO2	●	82.6	–		–		●	81.9	●	84.1	●
18OPEPO4	●	86.3	(●)	68.7	–		●	84.9	–		●
18OPEPO6	●	84.9	(●)	75.5	–		●	87.7	–		●
18OPEPO8	●	80.7	●	81.3	●	89.5	●	90.5	–		●
18OPEPO10	●	83.6	(●)	83.1	●	90.9	–		–		●
18OPEPO12	●	86.5	(●)	84.1	●	90.5	–		–		●
18OPEPO14	●	92.0	(●)	85.2	(●)	90.3	–		–		●
18OPEPO16	●	83.4	(●)	87.3	(●)	89.6	–		–		●
18OPEPO18	●	97.1	(●)	89.1	(●)	89.2	–		–		●
8OPEPO0	●	108.9	–		–		–		–		●
8OPEP2	●	51.2	–		–		(●)	39.8	(●)	49.7	●
8OPEP4	●	52.1	–		–		(●)	50.7	●	57.9	●
8OPEP6	●	53.4	–		–		●	59.3	●	63.4	●
8OPEP8	●	54.7	–		–		●	64.4	●	66.6	●
8OPEP10	●	56.2	–		–		●	66.9	●	68.0	●
8OPEP12	●	59.1	–		–		●	67.9	–		●
8OPEP14	●	61.7	–		–		●	67.6	–		●
8OPEP16	●	65.7	–		–		●	66.6	–		●
8OPEP18	●	71.7	–		–		(●)	65.1	–		●
8OPEP0	●	59.7	–		–		–		–		●
8OPPEP2	●	113.0	–		–		●	180.3	●	187.9	●

TABLE I (*Continued.*)

Compound	K		S_B	S_C	S_A		N		I
8OPPEP4	●	99.5	–	–	●	181.0	●	183.5	●
8OPPEP6	●	104.1	–	–	●	184.9	–		●
8OPPEP8	●	78.8	–	–	●	181.5	–		●
8OPPEP10	●	88.4	–	–	●	177.3	–		●
8OPPEP12	●	89.2	–	–	●	173.1	–		●
8OPPEP14	●	91.0	–	–	●	168.2	–		●
8OPPEP16	●	92.8	–	–	●	164.5	–		●
8OPPEP18	●	100.8	–	–	●	159.9	–		●

mesophase, despite the large range of variation of n and m (from 2 to 18) and despite the high sensitivity of the phase sequence to n and m. Figures 1 to 3 allow us to directly get an overview of the extension of these phenomena in the (n, m) plane: first, the variation of phase sequences (Fig. 1), second, the width of the enantiotropic liquid-crystalline domains ($T_{CL} - T_F$, T_{CL} and T_F being the clearing and the melting temperatures respectively, Fig. 2), and third, the width of the enantiotropic S_C domains ($T_{XC} - T_F$, Fig. 3). In Figure 1, different grey scales correspond to the different phase sequences. In Figure 2 and 3, solid lines join (n, m) values corresponding to an equivalent temperature range.

As is well known for calamitic materials, homologues with short chains show the nematic phase only. The increase of the chain lengths leads to the occurrence of disordered smectic phases (S_A and S_C), to the detriment of the nematic one; further increase stabilises ordered smectic phases. The domain of chain length explored includes almost all the homologues which are susceptible to exhibit disordered smectic phases: for example, the temperature range of the S_C phase is as narrow as 0.1 °C for the homologue (18OPEPO18) with the longest chains, and it is therefore highly probable that the corresponding terms with longer chains would not show such a disordered mesophase. As pointed out earlier[7], the S_A phase exists for intermediate chain lengths, the terms with slightly longer or shorter chains showing direct I-S_C or N-S_C transition respectively. In fact, there is a strong similarity in the occurrence of the successive mesophases (N-S_A-S_C-S_B), between the decrease of temperature for a given homologue and the increase of the chain length at constant temperature for an homologous series. This point will be analysed in detail on the basis of complementary measurements, later on[10].

In addition, the melting temperature is the lowest for the intermediate chain lengths, going from 52 °C for 8OPEPO6 to about 80 °C for 8OPEPO2 and 8OPEPO18, and 109 °C for 8OPEPO0. It is interesting to note that the chain lengths corresponding to the lowest melting point and to the largest extension of the S_A domain are very close, so that the largest S_A domain, or more generally the disordered smectic domains, and the largest enantiotropic liquid crystalline ranges are observed for almost the same homologues.

These comments about the influence of the chain length upon the polymorphism are very close to the conclusions of some earlier work[7], but need to be completed by a discussion of the influence of the chain length asymmetry $|n - m|$, the total chain

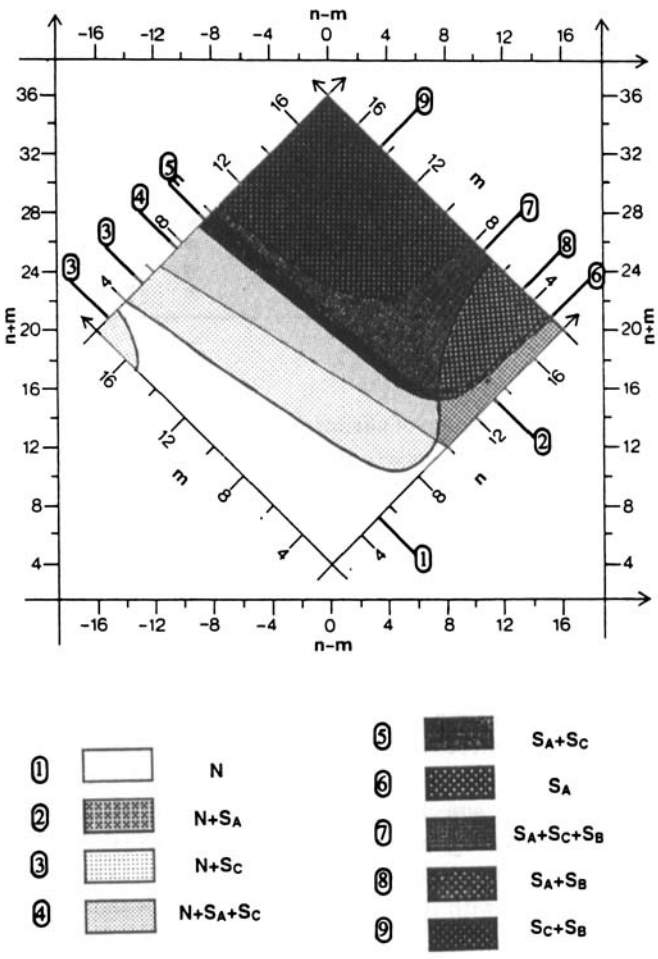

FIGURE 1 Stability domains of mesophases as a function of aliphatic chain lengths for the *n*OPEPO*m* homologues.

length $(n + m)$ being kept constant. Only the last point (number 10 in Reference 7) of these previous conclusions made a distinction between n and m, where the authors consider that "at least 6 carbon atoms on the acid chain are needed to see any smectic phase, no matter how long the chain on the phenolic side is". This point is not totally true, as the increase of n or m by taking the other parameter as constant always favours smectic phases to the deteriment of the nematic phase. For instance, 18OPEPO2 and 2OPEPO18 both show the N phase followed by a smectic phase with transition temperatures around 80 °C and a nematic range of about 2 °C; for the former homologue, the S_A phase follows a partially enantiotropic N phase; and for the latter homologue, the N phase precedes the S_C phase and is strongly monotropic. Concerning also the above comment[7], it is important to point out that the nematic phase is the only phase observed for homologues with $(n + m) < 10$.

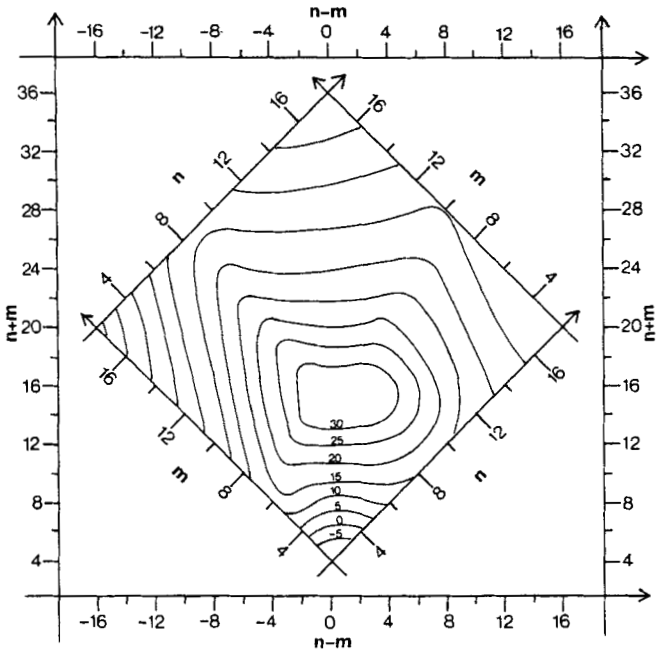

FIGURE 2 Variation of $T_{CL} - T_F$ as a function of aliphatic chain lengths for the *n*OPEPO*m* homologues.

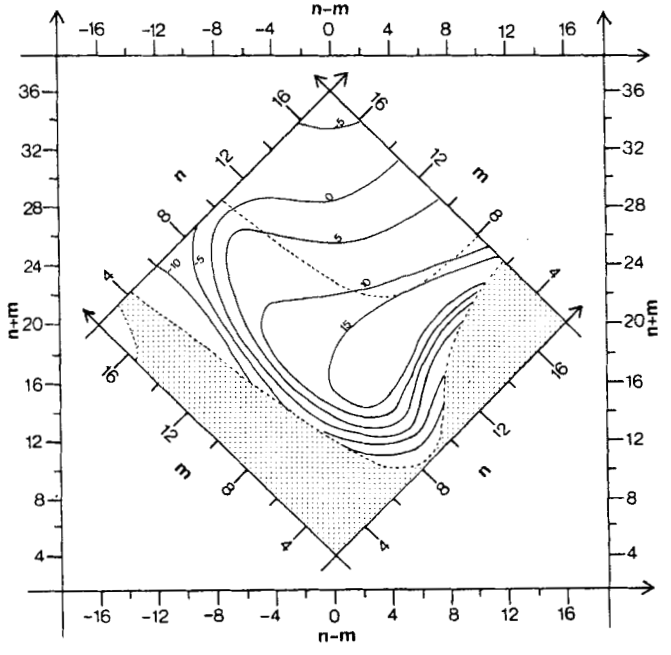

FIGURE 3 Variation of $T_{XC} - T_F$ as a function of aliphatic chain lengths for the *n*OPEPO*m* homologues.

As a matter of fact, the effect of increasing $|n - m|$ upon transition temperatures is the same for $n > m$ and $n < m$, consisting in an increase of the melting temperature and in a decrease of all the other transition temperatures. Furthermore, the variation of the clearing temperature is relatively small when compared with that of the nematic-disordered smectic transition temperatures. As a result, the enantiotropic domain shrinks and the nematic domain broadens. However, this schematic description needs to be moderated regarding some specific points:

- The lowest melting temperatures and the highest other transition temperatures are not observed for complete symmetric chains, but for n slightly larger than m (the optimal values of the chain asymmetry should be close to $(n - m) = 2$).
- Although the variation of the transition temperatures with $|n - m|$ shows the same trend for $(n - m)$ positive or negative, it is much steeper in the latter case and gives rise to a much more important variation of the enantiotropic and nematic domain sizes. In addition, the relative variations of the transition temperatures have not exactly the same amplitude in each case. This effect is particularly clear for the S_A-S_C transition in comparison with other transitions; as a consequence, the S_A phase is the only disordered smectic phase observed for very high $|n - m|$ values and for $(n - m) > 0$, while the narrow S_A temperature ranges observed for terms with symmetric chains of intermediate lengths vanish by increasing $(m - n)$.

As a conclusion of this part, our results, taken as a whole, agree with earlier descriptions concerning the influence of the chain length on the polymorphism. However, the above discussion shows that two parameters have to be considered together for a more precise analysis, i.e. the total chain length $(n + m)$, and the chain length asymmetry $|n - m|$. A molecular justification for using these parameters can be given *a posteriori*: indeed, it is well known that the amphipathic character due to the presence of polarisable rigid cores and of aliphatic chains strongly favours the micro-segregation and the formation of lamellar systems.[11] The smectic layering is then formed by the superposition of adjacent sublayers, respectively formed by the rigid cores, with a constant thickness, and by the alkyl chains, with a thickness proportional to $(n + m)$. In addition, the presence of chains of different length in one aliphatic sublayer, introduces some disorder, leading to some reduction of the transition temperatures.

It is clear that a deeper description, going beyond the influence of the chain length alone, would need a more extensive work including systematic variations of the rigid core structure. Nevertheless, the family of compounds, presented above, is obviously well suitable to perform an analysis of the relation between the polymorphism and the variation of the tilt angle in smectic C phases, as large areas of the (n, m) plane exist for each type of phase sequence: N-S_C, N-S_A-S_C, I-S_A-S_C and I-S_C.

2. TILT ANGLE VARIATION

a. Layer spacing, $d_A(n, m, T)$, in the smectic A phase

To obtain the value of the tilt angle, ψ, of the molecules in the S_C phase, it is necessary to know the value of the S_A layer spacing, d_A; when the S_A phase does not exist, d_A has to be

extrapolated from other values. In order to obtain this information, d_A has been represented at 80 °C as a function of $(n + m)$ in Figure 4 for the terms of *n*OPEPO*m* series. It is important to note that d_A increases linearly with $(n + m)$, without any significant influence of chain asymmetry. However, it has not been possible to take into account the temperature dependence effect of d_A, the S_A domains being too narrow in the *n*OPEPO*m* series.

To estimate the temperature effect on the layer spacing variation in the S_A phase of the compounds under consideration in the present work, it was decided to study similar derivatives exhibiting large S_A temperature ranges. So, the substitution of the alkoxy chain by an alkyl chain on the phenol side allowed us to destabilise the S_C phase, and the addition of a phenyl ring on the acid side resulted in the extension of the smectic A domain; therefore, the 8OPEP*m* and 8OPPEP*m* homologous series were considered. The variations of d_A for these two series (for which the synthesis and the liquid crystalline properties are also listed in Appendix I and Table I) are represented in Figure 5 as a function of $(n + m)$, at 50 °C and at 150 °C respectively. The corresponding average variation of the increase of d_A per methylene group as a function of temperature has then been introduced in the linear variation of d_A of *n*OPEPO*m* at 80 °C, shown in Figure 4. This results in the following expression of d_A as a function of the total aliphatic chain length and temperature:

$$d_A(\text{Å}) = 10.39 + 1.37(n + m) - 6.6\,10^{-4}(n + m)T$$

From this relation, it is clear that the temperature dependence effect (of the order of one tenth part of Å) could not be determined due the narrowness of the S_A temperature

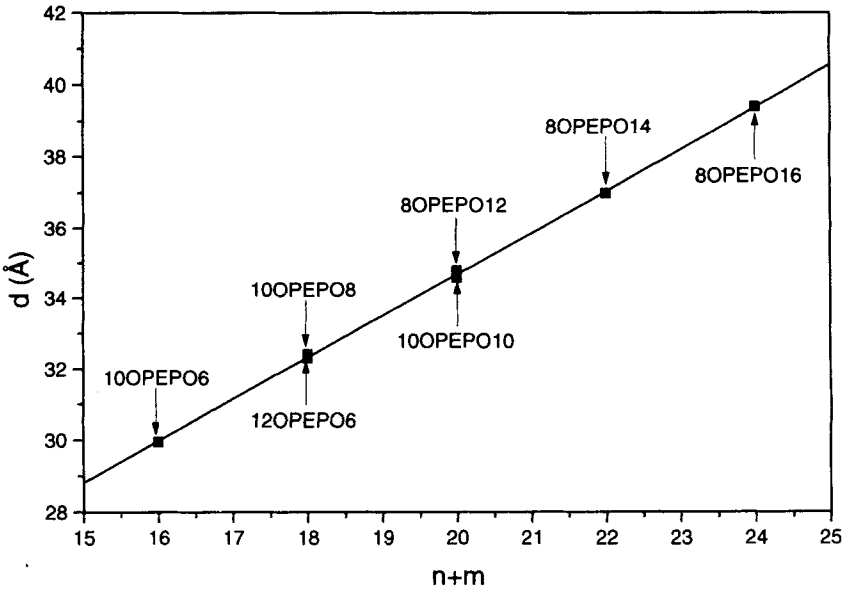

FIGURE 4 Variation of the smectic A layer spacing as a function of the total aliphatic chain length at 80 °C for the *n*OPEPO*m* homologues.

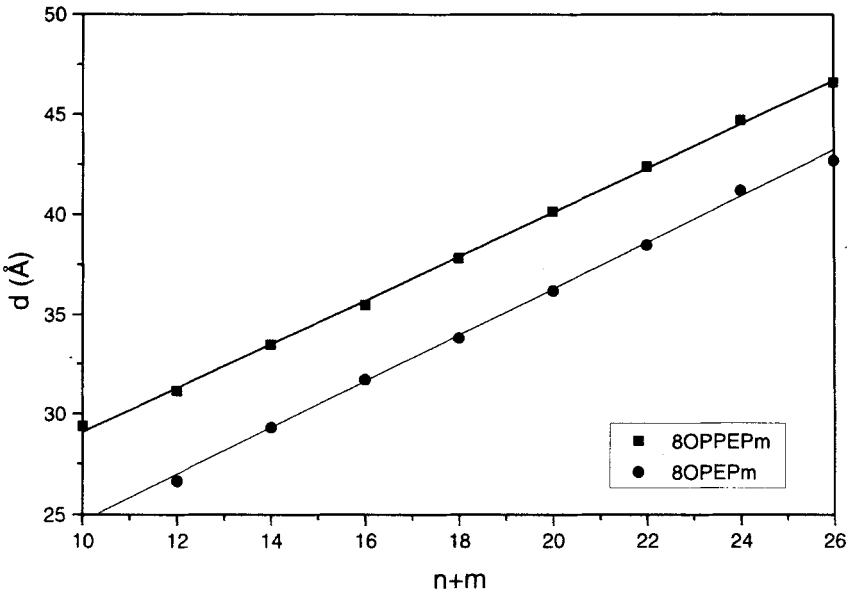

FIGURE 5 Variation of the smectic A layer spacing as a function of the total aliphatic chain length for the 8OPEP*m* homologues at 50 °C and for the 8OPPEP*m* homologues at 150 °C.

ranges in *n*OPEPO*m* homologues, with the only data at our disposal. In the smectic S_C phase, this temperature dependence is very small (almost negligible) with regard to that due to the tilt angle variation, and would not affect the comparison of $\psi(T)$ for different homologues of the series. Nevertheless, in order to minimize the error in the determination of ψ, it was decided to calculate the extrapolated values of d_A using the above relation.

b. Tilt angle, $\psi(n, m, T)$, in the smectic C phase

The ψ values have been calculated from the real values of the layer spacing, d_C, in the S_C phase and from those real (or virtual), d_A, in the S_A phase (see item **a**.). As the structure of the smectic C phase does not consist in rigid rods all tilted with the same angle in perfectly flat layers, it is clear that the definition of the tilt angle is ambiguous, and that different values can be obtained through different techniques, so that a combination of them is necessary to achieve a realistic model of tilting. However, the determination of the absolute tilt angle is not the topic the present work, which intends to describe its variation as a function of temperature and molecular parameters. The method used to determine the tilt angle ($\psi = \cos^{-1}(d_C/d_A)$ is one of the most used and gives highly reproducible data, without the difficulties related to the obtention of perfectly oriented samples, or to the estimation of correction factors.

The variations of ψ as a function of (n, m), at the transition from the I, N or S_A phase (temperature T_{XC}), at 2,5 and at 10 °C away from this transition, as well as at the low-temperature boundary of the S_C domain (see remarks below), are represented in

Figures 6 to 10, using the drawing technique described in the experimental section. They suggest the following comments:

α. Variation of ψ as a function of n and m at the transition

The ψ value is zero at the S_A-S_C transition, whereas it is non-zero at the I-S_C or N-S_C transition; this non-zero value becomes larger as the (n, m) compound is far from the S_A area in the (n, m) plane. The variation of ψ is particularly abrupt in the neighbourhood of the S_A area limits in the case of systems with I-S_C transition, where ψ increases from 0 to 20° for a very small increase in chain length; this variation is then considerably reduced up to a value of about 30 °C. Beyond this value, ψ increases only by 2° when the chain length increases by one methylene group.

When the S_C phase is preceded by a N phase, ψ varies slowly far from the S_A domain. Moreover, in this case, the asymmetry of aliphatic chains plays an important role, the variation of ψ being large when the chains are quite different in length.

Finally, the variation of ψ in the (n, m) plane is particularly important since ψ can reach a value of 32° at the N-S_C transition and 38° at the I-S_C transition.

β. Variation of ψ as a function of temperature

The variations of ψ with T follow the descriptions usually reported[12] for compounds presenting the S_A-S_C transition: the variations are steep close to the transition, and then

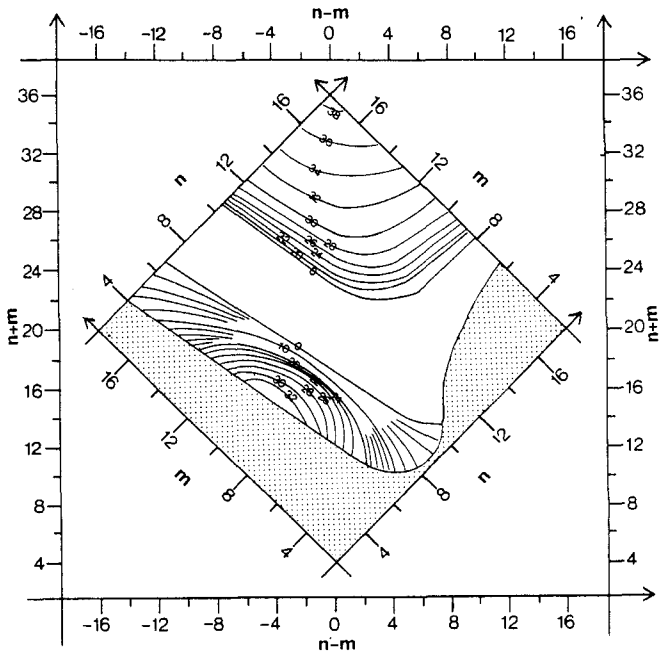

FIGURE 6 Variation of the tilt angle, ψ, with aliphatic chain length, at $T - T_{XC} = 0$ for the nOPEPOm homologues (the stippled domains are out of the smectic C domain).

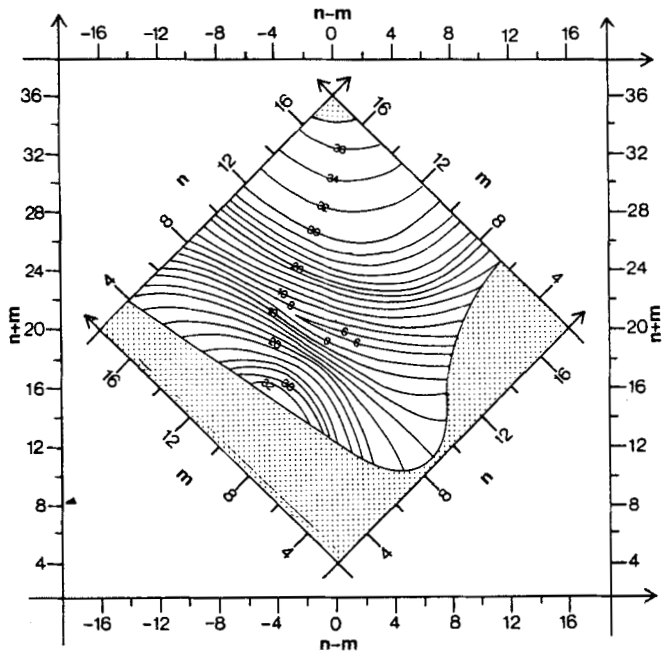

FIGURE 7 Variation of the tilt angle, ψ, with aliphatic chain length, at $T - T_{XC} = 2\,^{\circ}C$ for the *n*OPEPO*m* homologues (the stippled domains are out of the smectic C domain).

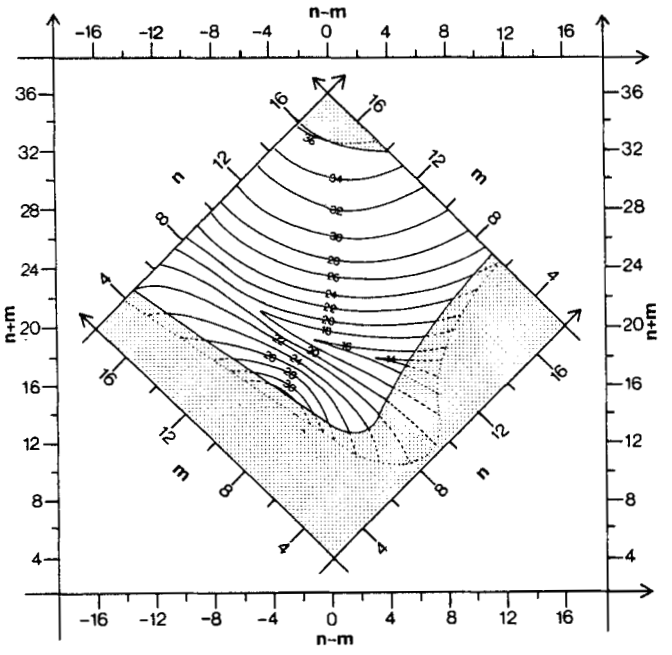

FIGURE 8 Variation of the tilt angle, ψ, with aliphatic chain length, at $T - T_{XC} = 5\,^{\circ}C$ for the *n*OPEPO*m* homologues (the stippled domains are out of the smectic C domain). The dotted lines indicate the boundaries of the smectic C domain when $T = T_{XC}$, and dashed lines extend the constant ψ lines towards these boundaries.

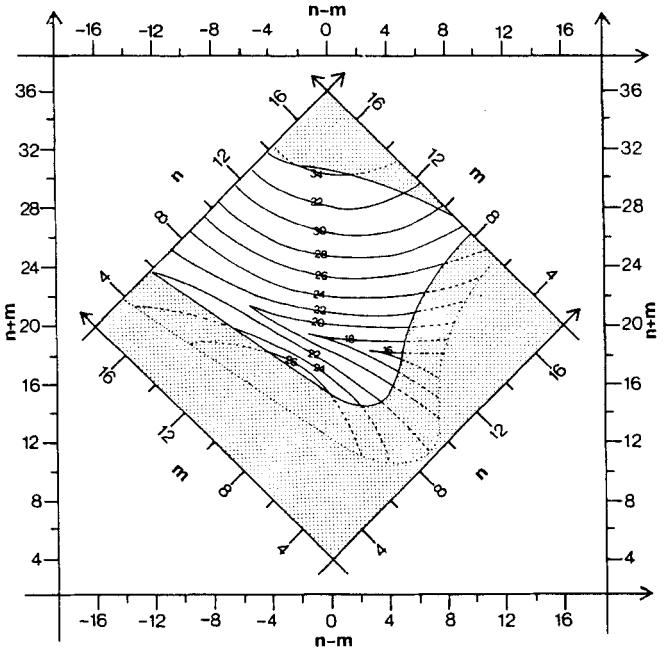

FIGURE 9 Variation of the tilt angle, ψ, with aliphatic chain length, at $T - T_{XC} = 10\,^{\circ}C$ for the *n*OPEPO*m* homologues (the stippled domains are out of the smectic C domain). The dotted lines indicate the boundaries of the smectic C domain when $T = T_{XC}$, and dashed lines extend the constant ψ lines towards these boundaries.

smoother and smoother when T decreases, resulting in an increase of ψ towards a saturation value.

However, a very large variation of the steepness of the variation of ψ with T towards its saturation value is observed in the n, m plane. So, when the S_C phase is preceded by a S_A phase, the slowest variation of ψ with temperature coincides with the presence of the widest S_A domain. Conversely, the variation of ψ becomes steeper when the S_A domain becomes narrower.

The same qualitative behaviour is observed beyond the limits of the S_A domain: the variation of ψ with T towards its saturation value becomes steeper as the distance to its boundaries increases. However, as the value at the transition also increases and approaches the saturation value, the variation of ψ in the S_C temperature range becomes *steadily* smaller, leading to a quasi temperature-independent tilt angle. Such variations can be described using the hypothesis of a virtual S_A phase with a virtual transition temperature T^*_{AC} above the N-S_C or I-S_C transition temperature T_{XC}; this concept has already been used in the case of optical textures studies[13], and in the case of studies about the evolution of polymorphism in binary mixtures.[9] Beyond the N-S_A-S_C- and I-S_A-S_C-boundaries, both the temperature range $(T^*_{AC} - T_{XC})$ and the steepness of the ψ variation near the virtual transition temperature increase continuously with T, lowering the residual variation of ψ in the real S_C temperature range, also continuously. Following this assumption, the evolution of $(T^*_{AC} - T_{XC})$ beyond

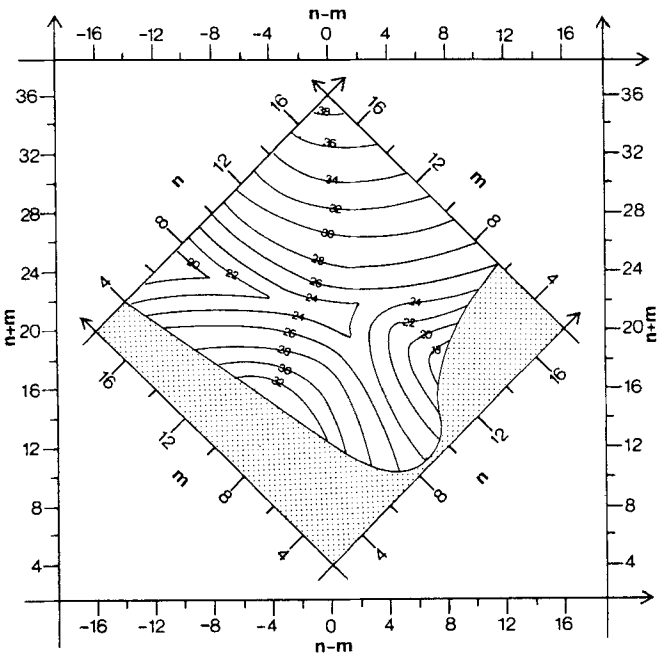

FIGURE 10 Variation of the maximum value in the (n, m) plane (the stippled domains are out of the smectic C domain).

the S_A-boundaries would be steeper for the I-S_C transition than for the N-S_C transition.

γ. Maximal value of ψ

Figure 10 represents the *approximate* variation of ψ_m in the (n, m) plane, ψ_m being the maximal value reached by ψ just before the crystallisation or the transition to the S_B phase. The estimated errors should not be larger than 2 to 3°, coming mainly from the large range of temperature considered in the extrapolation of the smectic A layer spacing (see relation in section *2.a*). On the other hand, the ambiguity about the definition of the crystallisation temperature has no significant influence on the ψ_m value since ψ is practically independent of temperature in the vicinity of the S_C phase boundary (the variation of ψ with T is slow when the width of the S_C domain is large).

The ψ_m variation in the (n, m) plane is similar to that of the ψ variation with T close to the transition: ψ_m is about 24 to 28° when the S_C phase exists with a S_A phase (or a little bit smaller for very dissymmetric homologues), while it goes up to 32 and 38°, when the S_C phase follows the N phase or the I phase respectively. It is interesting to note that ψ is nearly independent of temperature close to the low-temperature S_C phase boundary. This would mean that the optimal ψ value depends upon the length of the aliphatic chains, in contradiction with all models of the smectic C phase where the tilting is mainly attributed to interactions between the rigid cores of the molecules.

To conclude this part, the above representation of the ψ variation as a function of n, m and T clearly shows that it is not necessary to distinguish between several types of S_C phases, as it has often been reported in the literature[1]. On the contrary, the variations of ψ with T for compounds with N-S_C and I-S_C phase transitions can easily be described by assuming a virtual S_A-S_C transition at a temperature T^*_{AC}, located above the high-temperature limit of the S_C domain. In connection with this assumption, the variation of ψ with T becomes steadily steeper, when the temperature range $(T_{XA} - T_{AC})$ becomes narrow, or when the temperature range $(T^*_{AC} - T_{XC})$ becomes large $(X = N, I)$.

CONCLUSION

The transition temperatures determined in the present work for all the compounds belonging to the *n*OPEPO*m* homologous series are in good agreement with some available previous results. Nevertheless, we report a more precise description of the polymorphism by pointing out the influence of two parameters, the total chain length and the chain length asymmetry. It would, of course, be very interesting to vary other molecular features, like the magnitude of the off-axis dipole moments, in a further study.

The increase of the steepness of the ψ variation with T when the smectic A domain becomes smaller, already suggested from earlier studies (see introduction), is clearly observed again. This phenomenom can be extended to the homologues showing N-S_C and I-S_C transitions, with the assumption of a virtual transition temperature T^*_{AC}, obtained by the extrapolation of T_{AC} above the N-S_A-S_C and I-S_A-S_C triple lines. This assumption, also justified from binary mixtures studies, will be discussed in detail separately[9].

As a result of the increase of the difference between T^*_{AC} and T_{NC} or T_{IC} as a function of the distance to the S_A domain boundaries in the (n, m) plane, the value of ψ in the vicinity of the real transitions increases, and the residual variation of ψ in the S_C temperature range decreases, leading to an almost temperature-independent tilt angle. The fact that this process is continuous (for the homologues with I-S_C transitions, the evolution is steeper than for the ones with N-S_C transitions) indicates that the distinctions between several types of S_C phases, based on tilt angle temperature dependence[1], are irrelevant.

At the end of this work, it is now clearly established that there is an optimal value for the total chain length, close to the value corresponding to the widest mesomorphic temperature range, for which the width of the S_A domain is maximum and the steepness of the ψ variation with T, minimum. Increasing deviations from this optimal value induce increasing variations for these parameters. Based on further packing studies with complementary techniques, a discussion of this exciting observation will be performed in a forthcoming paper[10].

Acknowledgements

We thank Miss. Clarisse Luap, Alexandra Knaebel, Claire Marichal and Mr. Régis Chelly for their help in the characterisation of the materials.

References

1. A. De Vries, *J. Phys.*, **C1**, 1 (1975); De Vries A., Abstracts of the 5th International Liquid Crystal Conference, Stockholm, (1974).
2. G. Sigaud, F. Hardouin, M. F. Achard, *Solid State Comm.*, **23**, 35 (1977). D. Johnson, D. Allender, R. Dehoff, C. Maze, E. Oppenheim, R. Reynolds, *Phys. Rev.* **B 16**(1), 470 (1977).
3. C. Druon, J. M. Wacrenier, *Mol. Cryst. Liq. Cryst.*, **108**, 291 (1984).
4. G. R. Luckhurst, B. A. Timini, *Phys. Lett.*, **75A**, 91 (1979).
5. S. Krishna Prasad, V. N. Raja, D. S. S. Rao, G. G. Nair, M. E. Neubert, *Phys. Rev.* **A, 42**(4), 2479 (1990). Koden M. Anabuki, T. *Ferroelectrics*, **121**, 295 (1991).
6. S. C. Lien, C. C. Huang, *Phys. Rev.* **A, 30** (1), 624 (1984).
7. M. E. Neubert, T. T. Blair, Y. Dixon-Polverine, M. Tsai, C. C. Tsai, *Mol. Cryst. Liq. Cryst.*, **182B**, 269 (1990).
8. M. E. Neubert, T. Carlino, D. L. Fishel, D'Sidocki, *Mol. Cryst. Liq. Cryst.*, **59**, 253 (1980).
9. B. Heinrich, D. Guillon, to be published.
10. B. Heinrich, A. Skoulios, D. Guillon., to be published.
11. A. Skoulios, D. Guillon, *Mol. Cryst. Liq. Cryst.*, **165**, 317 (1988).
12. T. R. Taylor, J. L. Fergason, S. L. Arora, *Phys. Rev. Lett.*, **25** (11) 722, (1970). Doucet J., Levelut, A.-M., Lambert, M., *Mol. Cryst. Liq. Cryst.*, **24**, 317 (1973). Wise, R. A., Smith, D. H., Doane, J. W., *Phys. Rev.* **A, 7**(4), 1366 (1973).
13. M. Brunet, communication orale O-22, 5° Colloque d'Expression Francaise sur les Cristaux Liquides, Strasbourg, (1991); Petrov, M., Komitov, L., Simova, P., Hauck, G., *Phys. Stat. Sol.*, **A 89**, 451 (1985). Simova P., Petrov M., *Cryst. Res. Technol.*, **22**(4), 559 (1987); **22**(5), (1987) 737
14. P. Keller, L. Liebert, *Liq. Cryst. Sol. State Phys.*, Academic Press, New York, Supp. **14** (1978) 1; Amatore, Ch., Jutand, A., Negris, S., Fauvarque, J.-F., *Org. Chem.*, **390**, 389 (1990). V. Bhatt, J. Ramesh Babu, *Tet. Lett.*, **25**(32), 3497 (1984).

APPENDIX I: SYNTHESES

The procedures used were adapted from standard methods and from references [14]. All products were checked by ^{1}H-NMR and elemental analysis.

4-alkoxyphenols

To a solution of 2 mol. of hydroquinone and 1 mol. of 1-bromoalkane in 100 cm^3 of cyclohexanone was added 3 mol. of K_2CO_3. After the reaction mixture was refluxed for 12 hr, the hot suspension was filtered and the solvent removed by vacuum-distillation. The residue was dispersed in CH_2Cl_2 in order to separate the low-soluble hydroquinone. The crude mixture was filtered through a silica-gel column, using CH_2Cl_2 as an eluent, and then precipitated from pentane. The pure product was obtained by recrystallization, twice from a mixture of methanol/water ($R = C_2H_5$, C_4H_9, C_6H_{13}, C_8H_{17}), from absolute methanol ($R = C_{10}H_{21}$, $C_{12}H_{25}$, $C_{14}H_{29}$) or from absolute ethanol ($R = C_{16}H_{33}$, $C_{18}H_{37}$), and then, 3 times from a mixture of hexane/ CH_2Cl_2 ($R = C_2H_5$) or from pure hexane. Yields about 30–40% for phenols with short and intermediate chain lengths ($R = C_2H_5$ to $C_{12}H_{25}$), but only 20% for tetradecyloxyphenol, 8–10% for hexadecyloxyphenol and less than 5% for octadecyloxyphenol. ^{1}H-NMR for p-decyloxyphenol ($CDCl_3$): δ 0.89 (*t*, J7 Hz, 3H); δ 1.30 (*m*, 14H); δ 1.76 (*t*(*t*), J 8 Hz, 2H); δ 3.90 (*t*, J7 Hz, 2H); δ 4.50 (s, 1H); δ 6.77 (*s*, 4H).

4-alkylphenols

alkyl-4-hydroxyphenyl-ketone: alkanoylchloride, prepared from the acid and $SOCl_2$, is added dropwise to a mixture of 1 mol. of benzophenol, 3 mol. of $AlCl_3$ in 150 ml of nitrobenzene at 5–10°C for short chain length ($R = CH_3$, C_3H_7, C_5H_{11}, C_7H_{15}, C_9H_{19}), at room temperature for the C_{11}- and C_{13}-terms and at 40 °C and 50 °C for the C_{15}- and C_{17}-terms respectively. After 0.5 hr further stirring at 50 °C, the cooled solution is poured in a mixture of dilute H_2SO_4 and crushed ice. The organic layers were decanted or extracted with ether. The short terms (methyl- up to undecyl-hydroxyphenyl-ketone) were extracted from the organic mixture with dilute NaOH (15%). The aqueous phase was acidified with dilute H_2SO_4 and then extracted with ether. The separation of these homologues was completed by 2 further cycles of base-acid extractions. The higher terms were separated by crystallization, at first from the nitrobenzene solution and then 3 times from hexane. All the crude products were recrystallized, twice from ethanol or methanol and then twice from hexane or from a hexane/CH_2Cl_2 mixture, similar to the purification of 4-alkoxyphenols. Yields about 70–85%. ^{1}H-NMR for nonyl-4-hydroxyphenyl-ketone ($CDCl_3$): δ 0.88 (*t*, J 7 Hz, 3H); δ 1.30 (*m*, 12H); δ 1.73 (*t*(*t*), 2H); δ 2.93 (*t*, J7 Hz, 2H); δ6.26 (*s*, 1H); δ 6.91 (*d*, J 8Hz, 2H); δ7.92 (*d*, J 8 Hz, 2H).

One mol. of alkyl-4-hydroxyphenyl-ketone in 80 ml of ethanol was added to a suspension of 3 mol. of freshly prepared Zn-Hg-amalgam in 80 ml of 5N HCl. The mixture is then refluxed for 6–12 hr. The total conversion of the highest homologues ($R = C_{15}H_{31}$ and $C_{17}H_{35}$) required the same reduction to be repeated on the partial converted product, with fresh amalgam. After pouring the suspension into ice-water, the crude product was separated by means of an extraction with ether followed by filtering through a silica-gel column, using CH_2Cl_2 as an eluent. Further purifications were performed by recrystallizations, twice from ethanol or methanol and then twice from hexane or from a hexane/CH_2Cl_2 mixture, similar to the purification of 2. Yields: 80–90% for the homologues with intermediate and long chains, less than 70% for ethyl-, butyl- and hexyl-phenols. ^{1}H-NMR for p-decylphenol ($CDCl_3$): δ 0.89 (*t*, J7 Hz, 3H); δ 1.26 (*m*, 14H); δ1.57 (*t*(*t*), J 8Hz, 2H); δ2.53 (*t*, J 7 Hz, 2H);δ4.70 (*s*, 1H); δ 6.76 (*d*, J 8 Hz, 2H); δ 7.05 (*d*, J 8 Hz, 2H).

4-alkoxybenzoic acids

Methyl 4-alkoxybenzoates: to a solution of 1 mol. of methyl p-hydroxybenzoate and 1 mol. of 1- bromoalkane in 200 cm^3 of acetone was added 2 mol. of K_2CO_3. After the reaction mixture was refluxed for 6 hr, the hot suspension was filtered and the solvent removed by vacuum-distillation. The residue was dissolved in $CHCl_3$ and filtered through a plug of celite. The filtrate was washed twice with 3N HCl and twice with water. The crude mixture was filtered through a silica-gel column, using CH_2Cl_2 as an eluente. The pure product was obtained by recrystallization, twice in methanol or in a mixture of methanol/CH_2Cl_2 and once in hexane. Yields about 70%. ^{1}H-NMR for methyl 4-octyloxybenzoate ($CDCl_3$): δ 0.89 (*t*, J7 Hz, 3H); δ 1.29 (*m*, 10H); δ 1.81 (*t*(*t*), 2H); 3.98 (*s*, 3H); δ 4.04 (*t*, J7 Hz, 2H); δ7.03 (*d*, J 8 Hz, 2H); δ 8.13 (*d*, J 8 Hz, 2H).

To a mixture of 100 g of KOH, 25 g of water and 250 ml of methanol, was added 1 mol. of methyl 4-n-alkoxybenzoate. After the reaction mixture has been refluxed for

12 hr, the suspension was poured into ice-water and adjusted to pH 0-1 with dilute H_2SO_4. The acid suspension was filtered and washed with water and acetone. The crude product was dissolved in hot acetone, filtered, precipitated and then recrystallized twice in acetone. For C_{14}, C_{16} and C_{18}-homologues, ethyl acetate was used as a solvent instead of acetone. Yields about 90%. ^{1}H-NMR for p-octyloxybenzoic acid (DMSO-6D): δ 0.84 (*t*, J6 Hz, 3H); δ 1.24 (*m*, 10H); δ 1.70 (*t*(*t*), J 7 Hz, 2H); δ 4.00 (*t*, J7 Hz, 2H); δ 6.98 (*d*, J 8 Hz, 2H); δ 7.85 (*d*, J 8 Hz, 2H).

4-alkoxyphenyl and 4-alkylphenyl 4′-alkoxybenzoate

To a suspension of 0.1 mol. of alkoxybenzoic acid, 0.1 mol. of alkyl- or alkoxy-phenol and 0.01 mol. of DMAP in 100 ml of CH_2Cl_2, was added 0.2–0.3 mol. of DCC. After the reaction mixture has been stirred at room temperature for 2–3 hr, it was poured into 100 ml of 1N HCl and stirred at r.t. for 30 min. The suspension was filtered through a plug of celite. The ester was separated from the organic layers by filtering through a silica-gel column, using CH_2Cl_2 as an eluente. The crude product was recrystallized, twice from a mixture methanol/CH_2Cl_2, or ethanol/CH_2Cl_2 for homologues with long chains on the phenol-side, and twice from hexane or from a mixture of hexane/CH_2Cl_2. Yields about 70–80%, according to chain length. ^{1}H-NMR for 4-decyloxyphenyl-4′-octyloxybenzoate ($CDCl_3$): δ 0.90 (2*t*, J7 Hz, 6H); δ 1.29 (*m*, 24H); δ 1.81 (2*t*(*t*), 4H); δ 4.00 (*t*, J7 Hz, 2H); δ4.04 (*t*, J 7Hz, 2H); δ 7.03 (*d*, J 8 Hz, 2H); δ 7.10 (*d*, J 8 Hz, 2H); δ 7.15 (*d*, J 8 Hz, 2H); δ 8.13 (*d*, J 8 Hz, 2H). ^{1}H-NMR for 4-*n*-decylphenyl 4′-*n*-octyloxybenzoate ($CDCl_3$): δ 0.89 (*t*, J 7 Hz, 3H); δ0.90 (*t*, J 7 Hz, 3H); δ 1.29 (*m*, 26H); δ 1.82 (*t*(*t*), J 8 Hz, 2H); δ 2.62 (*t*, J 8 Hz, 2H); δ 4.04 (*t*, J 7 Hz, 2H); δ 6.96 (*d*, J 8 Hz, 2H); δ 7.09 (*d*, J 8 Hz, 2H); δ 7.22 (*d*, J 8 Hz, 2H); δ 8.13 (*d*, J 8 Hz, 2H).

4,4′-octyloxybiphenylcarboxylic acid

4,4′-methoxycyanobiphenyl: 4-methoxyphenyl magnesium bromide (1.5 mol.) was synthesized from 4-bromoanisole by the standard procedure using THF as a solvent. Direct coupling of the magnesium-derivative with the bromocyanobenzene is possible, but higher yield was obtained by using the organo-zinc derivative. The organo-zinc reagent was prepared by adding 3 mol. of crushed anhydrous zinc chloride to the corresponding Grignard reagent and by stirring the reagent mixture for 1 hr at room temperature. To this reagent, 1 mol. of bromocyanobenzene and 0.01 mol. of Pd° $(Pph_3)_4$ were added at 0 °C. After stirring for 30 min at 0 °C, the reaction mixture was kept at r.t. for 3-4 hr. At last, it was refluxed for 30 min. The cooled reaction mixture was poured into a mixture of dilute HCl and crushed ice. The organic layers were extracted with CH_2Cl_2 and filtered through a silica-gel column, using CH_2Cl_2 as an eluente. The crude product was precipitated several times from a mixture of hexane/CH_2Cl_2. The pure product was obtained by recrystallization, twice in a mixture of methanol/CH_2Cl_2 and twice in a mixture of hexane/CH_2Cl_2. Yield 60%. ^{1}H-NMR ($CDCl_3$): δ 3.86 (*s*, 1H); δ 6.97 (*d*, J 8 Hz, 2H); δ 7.49 (*d*, J 8 Hz, 2H); δ 7.66 (*s*, 4H).

4,4′-hydroxycyanobiphenyl: aluminium iodide was prepared by adding portionswise 3 mol. of I_2 to a suspension of 2 mol. of Al-powder in 250 ml of CH_3CN and refluxing the reaction mixture for 30 min. To this reagent, 1 mol. of 4,4′-methoxycyanobiphenyl

was added at r.t. and the mixture was refluxed for 4–5 hr. The suspension was poured into ice-water and adjusted to pH 0-1 with dilute H_2SO_4. The suspension was filtered and washed with water. The crude product was dissolved in ether. The organic layer was washed first with a $Na_2S_2O_3$ solution and then with water. After vacuum-distillation of the solvent, the crude product was recrystallized 3 times from $CHCl_3$. Yield 80%. ^{1}H-NMR (CD_3COCD_3): δ 4.14 (*s*, 1H); δ 6.97 (*d*, J 8 Hz, 2H); δ 7.49 (*d*, J 8 Hz, 2H); δ 7.66 (*s*, 4H)

4,4′-octyloxycyanobiphenyl: the O-alkylation of 4, 4′-hydroxycyanobiphenyl with 1-bromooctane and K_2CO_3 in acetone was performed with the same procedure as that used for methyl *p*-hydroxybenzoate. Yield 85%. ^{1}H-NMR ($CDCl_3$): δ 0.89 (*t*, J7 Hz, 3H); δ 1.32 (*m*, 10H); δ 1.82 (*t*(*t*), J 8 Hz, 2H); δ 4.01 (*t*, J7 Hz, 2H); δ 7.00 (*d*, J 8 Hz,2H); δ 7.53 (*d*, J 8 Hz, 2H); δ 7.64 (*d*, J 8 Hz, 2H); δ 7.70 (*d*, J 8 Hz, 2H).

To 3 kg of 25% of saturated KOH aqueous solution and 75% of isopropanol was added 1 mol. of 4,4′-octyloxycyanobiphenyl. After the reaction mixture has been refluxed for 30 min-1 hr, the nitrile was completely converted into the corresponding amide. However, the hydrolysis of the amide to the acid required 3-4 days refluxing. The suspension was poured into ice-water and adjusted to pH 0-1 with dilute H_2SO_4. The acid suspension was filtered and washed with water and acetone. The crude product was first recrystallized in ice-acetic acid and then dissolved in hot ethyl acetate, filtered, precipitated and recrystallized twice in ethyl acetate. Yield 85%. ^{1}H-NMR (DMSO-6D): δ 0.85 (*t*, J6 Hz, 3H); δ 1.26 (*m*, 10H); δ 1.71 (*t*(*t*), J7 Hz, 2H); δ 3.99 (*t*, J6 Hz, 2H); δ 7.02 (*d*, J 8 Hz, 2H); δ 7.66 (*d* J 8 Hz, 2H); δ 7.73 (*d*, J 8 Hz, 2H); δ 7.97 (*d*, J 8 Hz, 2H).

4″-alkylphenyl 4,4′-octyloxybiphenylcarboxylates

In this case, direct esterification methods from the acid failed or led to low yields, so that we used the classical condensation of the acid chloride in the presence of pyridine. 0.1 mol. of 4,4′-octyloxybiphenylcarboxylic acid and 300 ml of $SOCl_2$ were refluxed for 4 hr. The excess $SOCl_2$ was removed by vacuum-distillation. The acid chloride, dissolved in 100 ml of dry toluene was added portionswise to an ice-bath cooled solution of 0.15 mol. of alkylphenol in 150 ml of pyridine. After the reaction mixture has been stirred by cooling for 2 hr, it was poured into a mixture of dilute H_2SO_4 and crushed ice. The organic layers were extracted with ether and the residual pyridine was removed by extraction with dilute H_2SO_4. The crude product was separated by filtering through a silica-gel column, using CH_2Cl_2 as an eluente. Further purification was performed by the same procedure as for the esters of alkoxybenzoic acids. Yields 40–60%. ^{1}H-NMR for 4″-decylphenyl 4,4′-octyloxy-biphenylcarboxylate ($CDCl_3$): δ 0.89 (*t*, J7 Hz, 3H); δ 0.90 (*t*, J7 Hz, 3H); δ 1.28 (*m* 26H); δ 1.83 (*t*(*t*), J 8 Hz, 2H); δ 2.64 (*t*, J 8 Hz, 2H); δ 4.03 (*t*, J7 Hz, 2H); δ 7.01 (*d*, J 8 Hz, 2H); δ 7.13 (*d*, J 8 Hz, 2H); δ 7.25 (*d*, J 8 Hz, 2H); δ 7.61 (*d* J 8 Hz, 2H); δ 7.70 (*d*, J 8 Hz, 2H); δ 8.24 (*d*, J 8 Hz, 2H)